Is Weather Chaotic?

Coexisting Attractors, Multistability, and Predictability

by

Bo-Wen Shen[1,*], Roger A. Pielke Sr.[2], Xubin. Zeng[3],
Sara Faghih-Naini[1,4], Jialin Cui[1,5], and Robert Atlas[6]

[1]Department of Mathematics and Statistics, San Diego State University, San Diego, CA, USA
[2]CIRES, University of Colorado at Boulder, Boulder, CO, USA
[3]Department of Hydrology and Atmospheric Science, University of Arizona, Tucson, AZ, USA
[4]University of Bayreuth and Friedrich-Alexander University Erlangen-Nuremberg, Germany
[5]Department of Computer Sciences, San Diego State University, San Diego, CA, USA
[6]AOML, National Oceanic and Atmospheric Administration, Miami, FL, USA

[*]bshen@sdsu.edu

(To be submitted)
(Last Updated: 2020/09/12)

Abstract

Since Lorenz's 1963 study and 1972 presentation, the statement "weather is chaotic'' has been well accepted. Such a view turns our attention from regularity associated with Laplace's view of determinism to irregularity associated with chaos. In contrast to single type chaotic solutions, recent studies using a generalized Lorenz model (Shen 2019a, b; Shen et al. 2019) have focused on the coexistence of chaotic and regular solutions that appear within the same model, using the same modeling configurations but different initial conditions. The results suggest that the entirety of weather possesses a dual nature of chaos and order with distinct predictability. Furthermore, Shen et al. (2021a, b) illustrated the following two mechanisms that may enable or modulate attractor coexistence: (1) the aggregated negative feedback of small-scale convective processes that enable the appearance of stable, steady-state solutions and their coexistence with chaotic or nonlinear limit cycle solutions; and (2) the modulation of large-scale time varying forcing (heating).

Recently, the physical relevance of findings within Lorenz models for real world problems has been reiterated by providing mathematical universality between the Lorenz simple weather and Pedlosky simple ocean models, as well as amongst the non-dissipative Lorenz model, and the Duffing, the Nonlinear Schrodinger, and the Korteweg–de Vries equations (Shen 2020, 2021). We additionally compared the Lorenz 1963 and 1969 models. The former is a limited-scale, nonlinear, chaotic model; while the latter is a closure-based, physically multiscale, mathematically linear model with ill-conditioning. To support and illustrate the revised view, this short article elaborates on additional details of monostability and multistability by applying skiing and kayaking as an analogy, and provides a list of non-chaotic weather systems. We

additionally address the influence of the revised view on real-world model predictions and analyses using hurricane track predictions as an illustration, and provide a brief summary on the recent deployment of methods for multiscale analyses and classifications of chaotic and non-chaotic solutions.

Keywords: attractor coexistence, chaos, generalized Lorenz model, predictability, monostability, multistability

1. Introduction

Two studies of Prof. Lorenz (Lorenz 1963, 1972) laid the foundation of chaos theory that emphasize a Sensitive Dependence of Solutions on Initial Conditions (SDIC). While the concept of SDIC can be found in earlier studies (e.g., Poincare 1890), the rediscovery of SDIC in Lorenz (1963) changed our view on the predictability of weather and climate, yielding a paradigm shift from Laplace's view of determinism with unlimited predictability to Lorenz's view of deterministic chaos with finite predictability. Based on an insightful analysis of the Lorenz 1963 and 1969 (L63 and L69) models, as well as the recent development of generalized Lorenz models (GLM, Shen 2014, 2019a,b; Shen et al. 2019), such a conventional view is being revised to emphasize the dual nature of chaos and order given recent studies (Shen et al. 2021a,b).

To support and illustrate the revised view, this short article describes additional details for the following features: (1) Continuous vs. Sensitive Dependence on Initial Conditions (CDIC vs. SDIC); (2) single-types of attractors and monostability within the L63 model; (3) coexisting attractors and multistability within the GLM; (4) skiing vs. kayaking: an analogy for monostability and multistability; and (5) a list of non-chaotic weather systems. We additionally address the influence of the revised view on real-world model predictions and analyses by (6) viewing chaotic and non-chaotic solutions as steering flows in order to illustrate their impact on track predictions; (7) distinguishing instability, chaos, and computational chaos; (8) revealing saturation dependence on various types of solutions; and (9) providing a summary on the recent deployment of methods for analyzing scale interaction and detecting multistability.

2. Analysis and discussion

CDIC vs. SDIC

Figure 1 compares the time evolution of solutions from control and parallel runs that apply the same L63 model and parameters. The only difference in the two runs is that a tiny perturbation with $\epsilon = 10^{-10}$ was added into the initial condition of the parallel run. Both runs initially produce very close results but very different results at a later time. Initial comparable results indicate CDIC as an important feature of dynamic systems. Despite initial tiny differences, large differences in both runs, as indicated by the red and blue curves, appear at a later time. Such features are then referred to as SDIC, suggesting that a tiny change in an IC will eventually lead to a very different time evolution for a solution.

Single-types of attractors and monostability

Since Lorenz (1963), chaotic solutions have been a focal point for several decades, yielding the statement "weather is chaotic". In fact, depending on the relative strength of heating, the L63 model also produces non-chaotic solutions such as steady-state and limit cycle solutions (e.g., Figure 1 of Shen et al. 2021b). Given a model configuration, only one-type of solution, referred to as monostability, appears, as shown in Fig. 2 (left).

Coexisting attractors and multistability

By comparison, as shown in Fig. 2 (right), one of the major features within the GLM is so-called multistability with coexisting attractors. Two kinds of attractor coexistence include the 1st kind that contains coexisting chaotic and steady-state solutions and the 2nd kind that possesses coexisting, limit-cycle, and steady-state solutions. Such features occur in association with the coexistence of a saddle point and a stable critical point, enabled by the so-called aggregated

118 negative feedback of small-scale convective processes (Shen 2019a; Shen et al. 2021a). When a
119 time varying heating function that may represent a large-scale forcing system is applied, the first
120 and second kinds of attractor coexistence alternatively appear, leading to time varying
121 multistability. As a result of multistability, SDIC does not always appear.
122
123 **Monostability and multistability illustrated using skiing and kayaking**
124 To illustrate SDIC, Lorenz (1993) applied the activity of skiing (left in Fig 3) and developed
125 an idealized skiing model for revealing the sensitivity of time-varying paths to initial positions
126 (middle in Fig. 3). Based on the left panel, monostability appears when slopes are steep
127 everywhere. Namely, SDIC always appear. In comparison, the right panel for kayaking can be
128 used to illustrate multistability. In the photo, the appearance of strong currents and a stagnant area
129 (outlined with a white box) suggest instability and local stability, respectively. As a result, when
130 two kayaks move along strong currents, their paths display SDIC. On the other hand, when two
131 kayaks move into the stagnant area, they become trapped, showing no SDIC. Such features of
132 SDIC or no SDIC illustrate the nature of multistability. When currents change season by season,
133 time varying multistability is present.
134
135 **Non-chaotic weather systems**
136 The concept of multistability suggests the possibility for coexisting chaotic and non-chaotic
137 weather systems. Non-chaotic solutions have been previously applied for understanding the
138 dynamics of different weather systems, including steady-state solutions for investigating
139 atmospheric blocking (e.g., Charney and DeVore 1979; Crommelin et al. 2004), limit cycles for
140 studying 40-day intra-seasonal oscillations (Ghil and Robertson 2002), Quasi-Biennial

Oscillations (e.g., Renaud et al. 2019) and vortex shedding (Ramesh et. al. 2015), and nonlinear solitary-pattern solutions for understanding morning glory (i.e., a low-level roll cloud, Goler and Reeder 2004). Below, to illustrate its impacts on the movement of a tropical cyclone (TC), we present how a chaotic or non-chaotic, steady-state solution may be viewed as a "steering" flow.

Chaotic and non-chaotic solutions as steering flows

Three types of steering flows (associated with a saddle, a spiral source, or a spiral sink) are presented below and two kinds of track errors (Ivan-type vs. Sandy-type) are classified.

As discussed in Figure 1, a chaotic solution displays both CDIC and SDIC, corresponding to "regular" oscillation associated with a spiral source (Fig. 4a) and "irregular" oscillation associated with a saddle point (Fig. 4b), respectively. Zoomed-in views for an idealized spiral source and saddle point are provided in Figs. 5a and 5b, respectively. Although both critical points are unstable within the Lorenz 1963 model, the saddle point provides an essential ingredient for chaos. A trajectory near the spiral source may "regularly" move until it shifts away from the spiral source and towards the saddle point. Therefore, within the Lorenz 1963 model, a chaotic solution may display regular or irregular oscillations within short time intervals, depending on its location (i.e., near the spiral source or the saddle point). By comparison, the GLM allows for the coexistence of a stable spiral sink (as illustrated with an idealized stable spiral sink in Fig. 5c) and the saddle point. Hence, when a trajectory initially begins near the spiral sink, it may behave regularly during its entire lifetime. Such a scenario may occur when a kayak begins in a stagnant region (e.g., Fig 3).

Figure 5 displays three types of basic flows, including a spiral source, a saddle, and a spiral sink (from left to right). By viewing the "solutions" in Fig. 5 as steering flows, the above discussions suggest that flows associated with a spiral source or a spiral sink may lead to incremental changes of TC movement (or to incremental bias for TC track prediction), while a saddle point may lead to rapid changes of TC movement. From a perspective of steering flows, two types of TC track errors, as shown in Fig. 6, include: (i) an Ivan (2004)-type with a persistent track bias associated with an underestimated sub-tropical ridge (Stewart 2004; Shen et al. 2006) and (ii) a Sandy (2012) type with rapid diverged tracks associated with a steering flow that contains a saddle point (Blake et al. 2013; Shen et al. 2013). Very slight differences determine whether a TC (e.g., Sandy) recurves to the northeast, or wraps back west.

The above discussions suggest that improving these track predictions requires an analysis of the location and intensity (i.e., intensification or weakening) of a subtropical ridge and/or "predicting" the potential for the appearance of a saddle point, (e.g., whether two large-scale systems that move in an opposite direction may approach one other).

Instability, Chaos, and Computational Chaos

Simple definitions of instability and chaos are defined as follows: (1) instability is defined as an unbounded amplification; and (2) chaos is defined as a bounded, time-varying, growing solution that requires solution boundedness and, at least, one positive Lyapunov exponent (LE, Wolf et al. 1985; Shen 2014, 2019a). Such a definition with a positive LE and boundedness is consistent with the definition of chaos that is based on SDIC,

Strictly speaking, instability (or stability) dominates when an orbit is near the spiral source (or the spiral sink). Such dynamics are less complicated as compared to chaotic dynamics. Namely, better predictability is expected. Chaotic dynamics become important or dominate when an orbit moves closer to a saddle point. (Note that the above discussions are based on two-dimensional, unstable, spiral critical points. Within the three-dimensional phase space, an unstable non-trivial critical point may contain a 2D spiral source and a stable manifold in the 3rd dimension, appearing as a special kind of saddle that complicates the dynamics and, thus, discussions).

In Lorenz (1989, 2006), the term computational chaos was introduced for indicating the appearance of chaotic responses associated with large time steps. Such a feature can be illustrated using the logistic equation (Eq. 1) and the logistic map (Eqs. 2a-2c), as shown below:

$$dX/d\tau = rX\,(1 - X), \qquad (1)$$

$$Y_{n+1} = \rho Y_n\,(1 - Y_n), \qquad (2a)$$

$$Y_n = r\Delta\tau X_n/(1 + r\Delta\tau), \qquad (2b)$$

$$\rho = 1 + r\Delta\,\tau. \qquad (2c)$$

Here, τ represents the time variable and $\Delta\tau$ represents the time step. The two time-dependent variables are X and Y, and the two time-independent parameters are r and ρ. Eq. (2) is obtained from Eq. (1) using a forward finite difference scheme. Therefore, while Eq. (1) is continuous in

time, Eq. (2) is discrete in time. As summarized in Table 1, Eq. (1) contains an analytical, non-chaotic solution and Eq. (2) produces bifurcation and chaos at a large parameter, ρ, requiring a large $\Delta\tau$ as a result of Eq. (2c). Therefore, "irregular responses" in Eq. (2) may be viewed as computational chaos. Similarly, such a feature of bifurcation was previously documented using a discrete version of the equation for terminal velocities (e.g., Shen and Lin 1995).

Saturation dependence on various types of solutions

Within nonlinear chaotic solutions, root-mean-square (RMS) forecast errors may approach constants as time proceeds, being saturated when sufficiently large ensemble runs are applied. Since all of the steady-state solutions eventually become constant, their RMS errors may appear saturated. In contrast, nonlinear oscillatory solutions may produce oscillatory RMS errors (e.g., Liu et al. 2009). On the other hand, nonlinear oscillatory solutions may appear as computational chaos, displaying saturation, when insufficient temporal solutions are used. Therefore, saturated RMS errors should not be used as a sole indicator for revealing the chaotic nature of weather.

Methods for analyzing scale interaction and detecting multistability

The above discussions suggest that an effective detection of scale modulation and/or non-chaotic solutions may lead to better predictability, thereby improving our confidence in numerical weather and climate predictions. In our recent studies, in addition to the "standard" method for computing Lyapunov Exponents (LEs) within five- and nine-dimensional Lorenz models (Shen 2014, 2019a), the following methods have been deployed: (1) the Parallel Ensemble Empirical Mode Decomposition (PEEMD) for revealing scale interactions (Wu and Shen 2016; Shen et al. 2017); (2) Recurrence Plots (RPs) for the analysis of multiple African easterly waves that display

differences in phases and amplitudes (Reyes and Shen 2019; 2020); and (3) a Kernel Principal Component Analysis (K-PCA) for separating chaotic and non-chaotic attractors (Cui and Shen 2021).

3. Concluding Remarks

In the past, Lorenz models have been applied in order to reveal the chaotic and unstable nature of weather and climate and to understand the intrinsic predictability of weather and climate, as well as the practical predictability of models and initial conditions. Based on this report and recent studies, an insightful analysis of the classical Lorenz 1963 and 1969 models and development of the generalized Lorenz model (GLM) suggest the following:

- The Lorenz 1963 nonlinear model with monostability is effective for revealing the chaotic nature of weather, suggesting finite intrinsic predictability.
- The Lorenz 1969 model is a closure-based, physically multiscale, mathematically linear model with ill-conditioning; it easily captures numerical instability and, thus, is effective for revealing finite predictability.
- The GLM with coexisting attractors and multistability suggests both limited and unlimited intrinsic predictability.
- Using selected cases within a global model (e.g., Shen 2019b), a practical predictability of 30 days was previously documented.

Given the above results, we previously proposed a revised view on the dual nature of chaos and order with distinct predictability in weather and climate.

To support and illustrate the revised view, here, we elaborated on additional details for monostability and multistability by applying skiing and kayaking as an analogy and by providing a list of non-chaotic weather systems. We further extended related studies in order to address the influence of the revised view on real-world model predictions and analyses. By viewing chaotic and non-chaotic solutions as steering flows, we identified two-types of track errors, including an Ivan (2004)-type and a Sandy (2012)-type, whose movements were impacted by a spiral source (as a subtropical ridge) and a saddle point, respectively. The former should be more predictable.

We additionally discussed differences surrounding instability, chaos, and computational chaos, and illustrated the saturation dependence on various types of solutions. While saturated RMS errors may indicate either chaos or computational chaos, oscillatory RMS errors are likely associated with nonlinear oscillatory solutions. We finally provided a summary on the recent deployment of methods (e.g., PEEMD, RP, and K-PCA) for multiscale analyses and classifications of chaotic and non-chaotic solutions with the aim of identifying systems with better predictability.

Availability of data and material

Source codes of Lorenz models are available upon request.

Competing interests

The authors declare no competing interest.

Funding

N/A

Authors' contributions

Shen designed and performed research; Shen, Pielke, Zeng, and Atlas wrote the paper; Shen, Faghih-Naini, and Cui analyzed the equations and produced plots

ACKNOWLEDGEMENTS

We thank Drs. F. Marks, S. Gopalakrishnan (of NOAA/AOML), and S.-C. Yang (of NCU) for valuable comments and discussions on the application of related studies for hurricane prediction.

References

Blake ES, Kimberlin TB, Berg RJ, Cangiaolsi JP, Beven JL II (2013) Tropical cyclone report: Hurricane Sandy, Rep. AL182012. Natl Hurricane Cent, Miami, Florida, USA.

Charney, J. G., and J. G. DeVore, 1979: Multiple flow equilibria in the atmosphere and blocking. J. Atmos. Sci., 36, 1205–1216.

Crommelin, D.T., J.D. Opsteegh, and F. Verhulst, 2004: A mechanism for atmospheric regime behavior, J. Atmos. Sci. 61 (2004) 1406–1419.

Cui, J. and B.-W. Shen, 2021: A Kernel Principal Component Analysis of Coexisting Attractors within a Generalized Lorenz Model. Chaos, Solitons & Fractals, 146. https://doi.org/10.1016/j.chaos.2021.110865.

Ghil, M., A.W. Robertson, 2002: "Waves" vs. "particles" in the atmosphere's phase space: A pathway to long-range forecasting? Proceedings of the National Academy of Sciences Feb 2002, 99 (suppl 1) 2493-2500; DOI: 10.1073/pnas.012580899

Goler, R. A., and M. J. Reeder, 2004: The generation of the morning glory, J. Atmos. Sci., 61(12), 1360–1376.

Liu, H.-L., F. Sassi, and R. R. Garcia, 2009: Error growth in a whole atmosphere climate model. J. Atmos. Sci., 66, 173–186, https://doi.org/10.1175/2008JAS2825.1.

Lorenz, E. N., 1963: Deterministic nonperiodic flow, J. Atmos. Sci., 20, 130-141.

Lorenz, E. N., 1969: The predictability of a flow which possesses many scales of motion. Tellus, 21, 289–307.

307 Lorenz, E. N., 1972: Predictability: Does the flap of a butterfly's wings in Brazil set off a tornado
308 in Texas? Proc. 139th Meeting of AAAS Section on Environmental Sciences, New Approaches
309 to Global Weather: GARP, Cambridge, MA, AAAS, 5 pp.
310 Lorenz, E. N., 1993: The Essence of Chaos. University of Washington Press, Seattle, 227pp.
311 Lorenz, E. N., 1989: Computational chaos: A prelude to computational instability. Physica D, 35D,
312 299–317, https://doi.org/10.1016/0167-2789(89)90072-9.
313 Lorenz, E. N., 2006: Computational periodicity as observed in a simple system. Tellus, 58A, 549–
314 557, https://doi.org/10.1111/j.1600-0870.2006.00201.x.
315 Poincaré, H. (1890). Sur le problème des trois corps et les équations de la dynamique. Acta
316 Mathematica, 13, 1-270.
317 Ramesh, K., J. Murua, A. Gopalarathnam, 2015: Limit-cycle oscillations in unsteady flows
318 dominated by intermittent leading-edge vortex shedding. Journal of Fluids and Structures,
319 Volume 55, 84-105.
320 Renaud, A., L.-P. Nadeau, and A. Venaille, 2019: Periodicity Disruption of a Model Quasibiennial
321 Oscillation of Equatorial Winds. PHYSICAL REVIEW LETTERS 122, 214504 (2019).
322 Reyes, T., and B.-W. Shen, 2019: A recurrence analysis of chaotic and non-chaotic solutions
323 within a generalized nine-dimensional Lorenz model. Chaos Solitons Fractals, 125, 1–12,
324 https://doi.org/10.1016/j.chaos.2019.05.003.
325 Reyes, T. and B.-W. Shen, 2020: A Recurrence Analysis of of Multiple African Easterly Waves
326 during Summer 2006, Current Topics in Tropical Cyclone Research, Anthony Lupo,
327 IntechOpen, DOI: 10.5772/intechopen.86859.
328 Shen, B.-W., 2014: Nonlinear Feedback in a Five-dimensional Lorenz Model. J. of Atmos. Sci.,
329 71, 1701–1723. doi:http://dx.doi.org/10.1175/JAS-D-13-0223.1

330 Shen, B.-W., 2019a: Aggregated Negative Feedback in a Generalized Lorenz Model. International
331 Journal of Bifurcation and Chaos, Vol. 29, No. 3 (2019) 1950037.
332 https://doi.org/10.1142/S0218127419500378
333 Shen, B.-W., 2019b: On the Predictability of 30-day Global Mesoscale Simulations of Multiple
334 African Easterly Waves during Summer 2006: A View with a Generalized Lorenz Model.
335 Geosciences 2019, 9(7), 281; https://doi.org/10.3390/geosciences9070281
336 Shen, B.-W., 2020: Homoclinic Orbits and Solitary Waves within the non-dissipative Lorenz
337 Model and KdV Equation. International Journal of Bifurcation and Chaos. 30. 2050257-1-15.
338 DOI:10.1142/S0218127420502570
339 Shen, B.-W., 2021: Solitary Waves, Homoclinic Orbits, and Nonlinear Oscillations within the non-
340 dissipative Lorenz Model, the inviscid Pedlosky Model, and the KdV Equation. In: Christos H.
341 Skiadas, Yiannis Dimotikalis (eds) The 13th Chaos International Conference CHAOS 2020.
342 Springer Proceedings in Complexity. Springer, Cham. (in press)
343 Shen, B.-W., and N.-H. Lin, 1995: A Theoretical Study of the Effects of an Isolated Mountain on
344 Particle Deposition. J. of Atmos. Sci., 23, Taipei, Taiwan (in Chinese), 237-264.
345 Shen, B.-W.*, R. Atlas, J.-D. Chern, O. Reale, S.-J. Lin, T. Lee, and J. Chang, 2006: The 0.125
346 degree Finite Volume General Mesoscale Circulation Model: Preliminary simulations of
347 mesoscale vortices. Geophys. Res. Lett., 33, L05801, doi:10.1029/2005GL024594.
348 Shen, B.-W.*, M. DeMaria, J.-L. F. Li, and S. Cheung, 2013: Genesis of Hurricane Sandy (2012)
349 Simulated with a Global Mesoscale Model. Geophys. Res. Lett. 40. 2013, DOI:
350 10.1002/grl.50934.
351 Shen, B.-W., S. Cheung, Y. Wu, F. Li, and D. Kao, 2017: Parallel Implementation of the Ensemble
352 Empirical Mode Decomposition (PEEMD) and Its Application for Earth Science Data Analysis.

353 Computing in Science & Engineering, vol. 19, no. 5, pp. 49-57, September/October 2017,
354 doi:10.1109/MCSE.2017.3421555.
355 Shen, B.-W., T. A. L Reyes and S. Faghih-Naini, 2019: Coexistence of Chaotic and Non-Chaotic
356 Orbits in a New Nine-Dimensional Lorenz Model. In: Skiadas C., Lubashevsky I. (eds) 11th
357 Chaotic Modeling and Simulation International Conference. CHAOS 2018. Springer
358 Proceedings in Complexity. Springer, Cham. https://doi.org/10.1007/978-3-030-15297-0_22
359 Shen, B.-W., Pielke, R. A., Sr., Zeng, X., Baik, J.-J., Faghih-Naini, S., Cui, J. & Atlas, R., 2021a
360 "Is weather chaotic? Coexistence of chaos and order within a generalized Lorenz model," Bull.
361 Amer. Meteor. Soc., 1–28, https://doi.org/10.1175/BAMSD-19-0165.1
362 Shen, B.-W., R. A. Pielke Sr., X. Zeng, J.-J. Baik, S. Faghih-Naini, J. Cui, R. Atlas, and T.A.
363 Reyes, 2021b: Is Weather Chaotic? Coexisting Chaotic and Non-Chaotic Attractors within
364 Lorenz Models. In: Christos H. Skiadas, Yiannis Dimotikalis (eds) The 13th Chaos International
365 Conference CHAOS 2020. Springer Proceedings in Complexity. Springer, Cham. (in press)
366 Stewart, S. R., 2004: Tropical Cyclone Report. Natl Hurricane Cent, Miami, Florida, USA.
367 Wu, Y.-L., and B.-W. Shen, 2016: An evaluation of the parallel ensemble empirical mode
368 decomposition method in revealing the role of downscaling processes associated with African
369 easterly waves in tropical cyclone genesis. J. Atmos. Oceanic Technol., 33, 1611–1628,
370 https://doi.org/10.1175/JTECH-D-15-0257.1.
371 Wolf, A., Swift, J. B., Swinney, H. L. & Vastano, J., 1985: "Determining Lyapunov exponents
372 from a time series," Physica D 16, 285–317.
373

Table 1: Computational chaos illustrated using the Logistic equation (Eq.) and the Logistic map in Eqs. (1) and (2).

Name	Type	Solution	Eq.
Logistic Eq.	differential	analytical, non-chaotic	(1)
Logistic map	difference	chaotic at large time steps	(2)

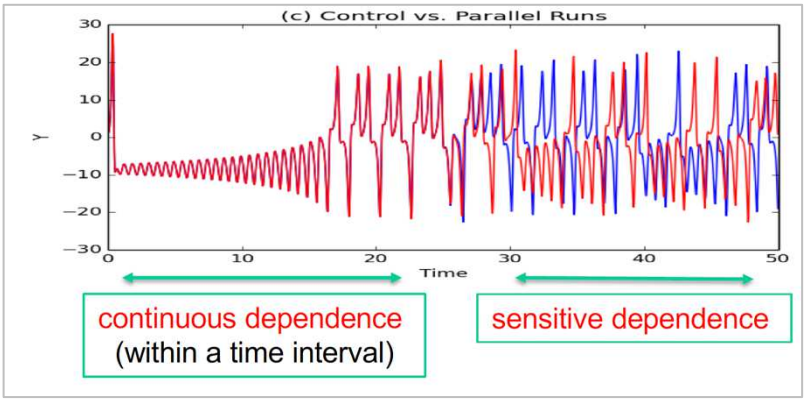

Fig. 1. An illustration of sensitive dependence on initial conditions (SDIC) and solution boundedness within the Lorenz model. Control and parallel runs were performed using the same model and the same model parameters. The only difference between the two runs is the inclusion of an initial tiny perturbation within the parallel run, $\varepsilon = 10^{-10}$. As shown with the red curve, the two runs initially produced almost the same result for $\tau \in [0, 25]$. This feature is called "Continuous Dependence on Initial Conditions" (CDIC). During longer time integrations, the appearance of two curves (in red and blue) indicates significant differences (i.e., "rapid divergence") of solutions for the control and parallel runs. Such a feature is then called SDIC, due to the initial tiny perturbation, $\varepsilon = 10^{-10}$. Boundedness is indicated by the finite values of solutions.

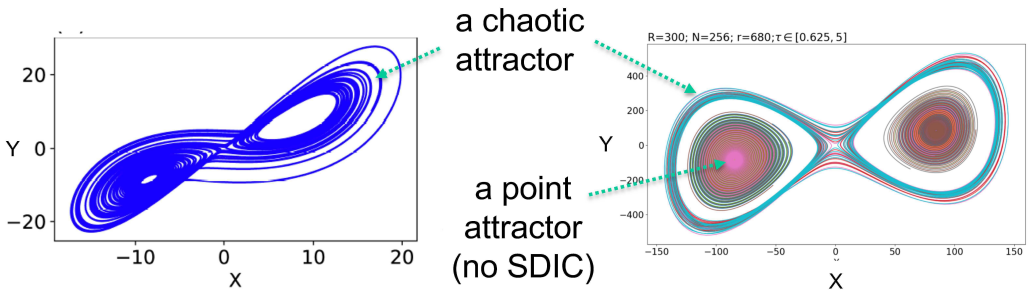

Fig. 2: Monostability illustrated by the chaotic solution of the L63 model (left), and multistability by coexisting chaotic and steady-state solutions of the GLM (right).

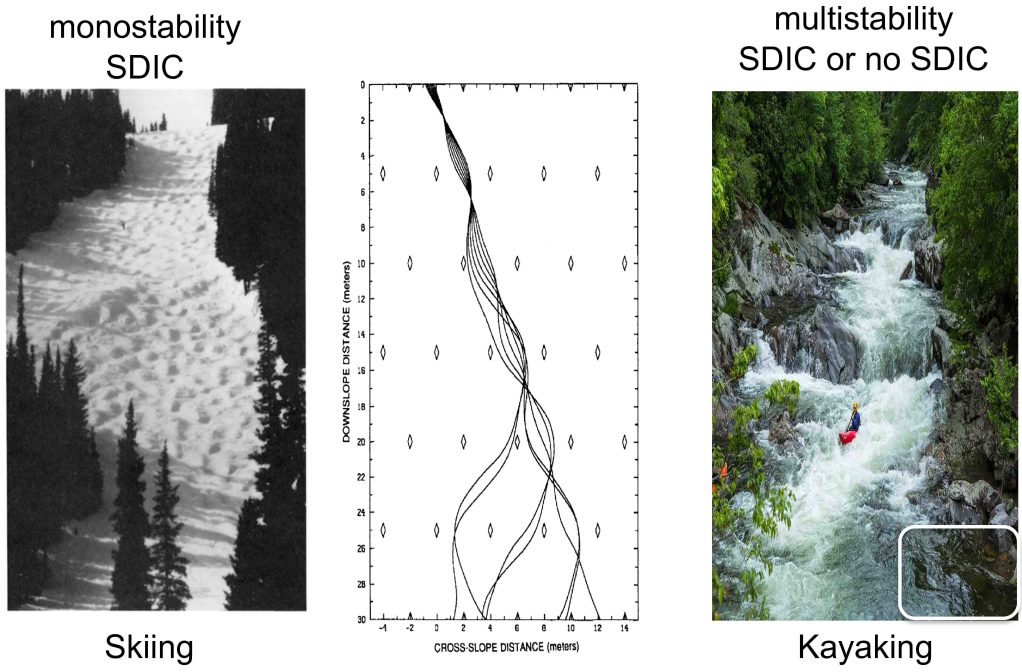

Fig. 3: Skiing as used to reveal monostability (left and middle, Lorenz 1993) and kayaking as used to indicate multistability (right, Copyright: ©Carol- stock.adobe.com). A stagnant area is outlined with a white box.

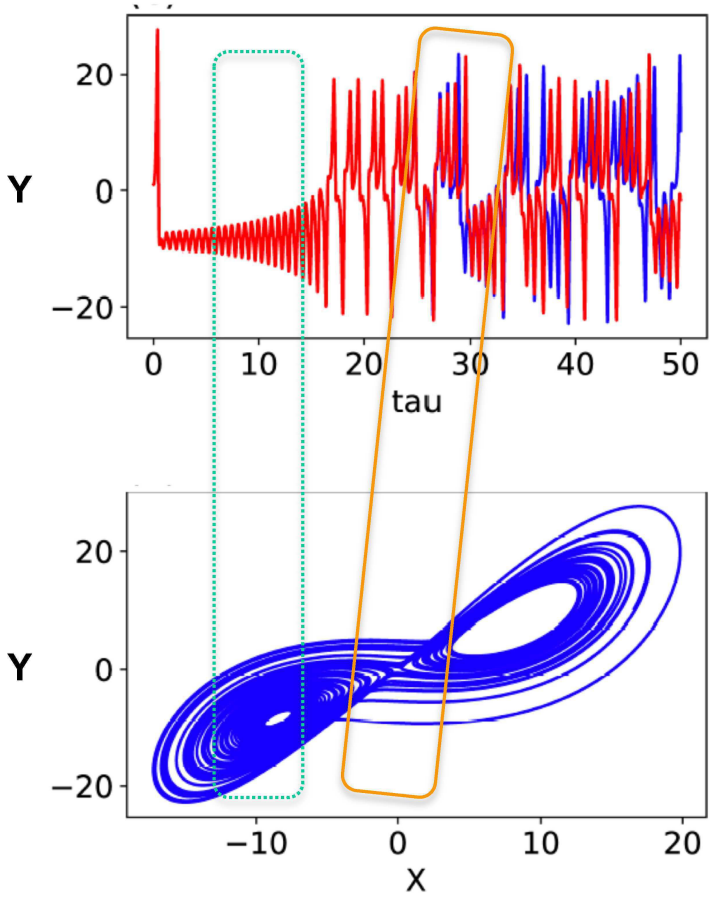

Fig. 4: A time-varying chaotic solution within the Lorenz 1963 model (top) and its two-dimensional phase portrait (bottom). A green (orange) box indicates the association of regular (irregular) oscillation with a spiral source (a saddle).

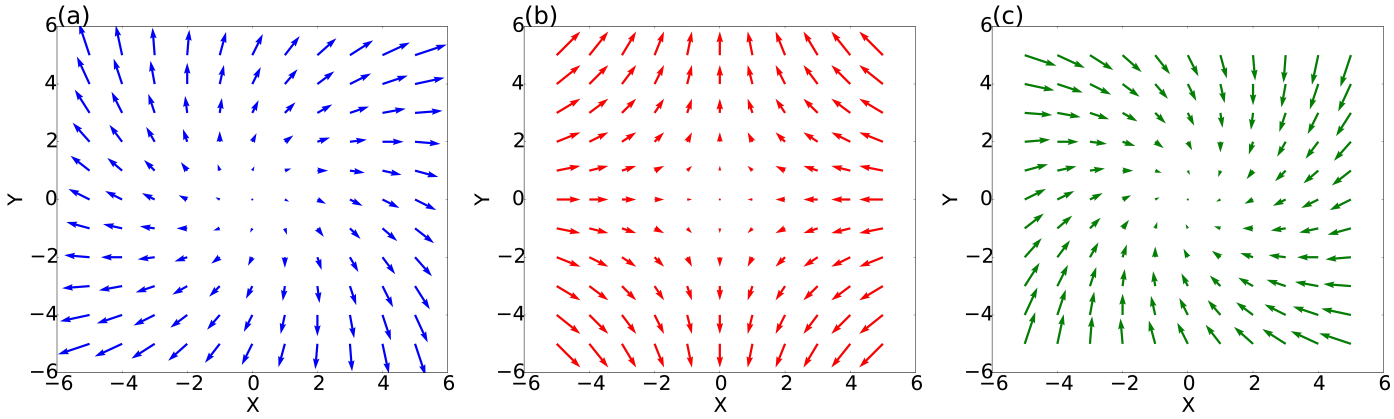

Fig. 5: Three basic types of solutions, including a spiral source (a), a saddle (b), and a spiral sink (c).

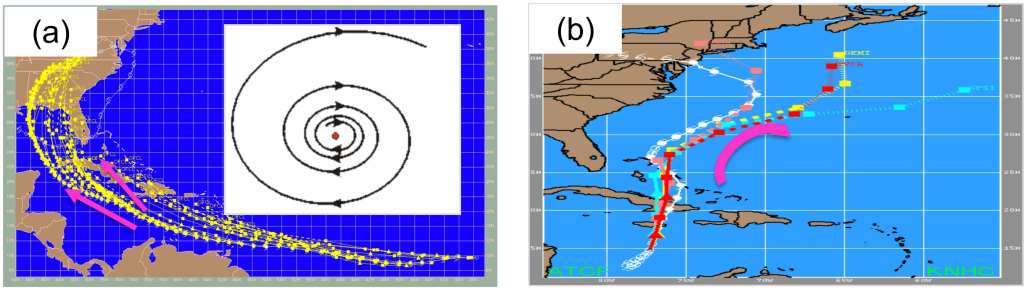

Fig. 6: Two types of track errors associated with different steering flows. (a) Hurricane Ivan (2004) (e.g., Stewart 2004) and (b) Hurricane Sandy (2012) (e.g., Blake et al. 2013).